

# In Situ Spectroscopic Examination of a Low Overpotential Pathway for Carbon Dioxide Conversion to Carbon Monoxide

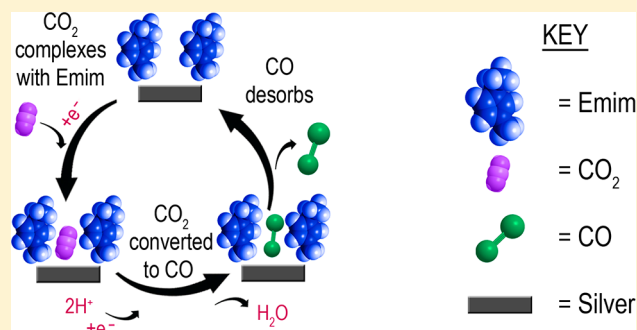
Brian A. Rosen,<sup>†,‡</sup> John L. Haan,<sup>‡,§</sup> Prabuddha Mukherjee,<sup>§</sup> Björn Braunschweig,<sup>§</sup> Wei Zhu,<sup>†</sup> Amin Salehi-Khojin,<sup>†</sup> Dana D. Dlott,<sup>§</sup> and Richard I. Masel<sup>\*,†</sup>

<sup>†</sup>Dioxide Materials, 60 Hazelwood Drive, Champaign, Illinois 61820, United States

<sup>‡</sup>Department of Chemical and Biomolecular Engineering and <sup>§</sup>Department of Chemistry, University of Illinois, 600 South Mathews Avenue, Urbana, Illinois 61801, United States

## S Supporting Information

**ABSTRACT:** Lowering the overpotential for the electrochemical conversion of CO<sub>2</sub> to useful products is one of the grand challenges in the Department Of Energy report, “Catalysis for Energy”. In a previous paper, we showed that CO<sub>2</sub> conversion occurs at low overpotential on a 1-ethyl-3-methylimidazolium tetrafluoroborate (EMIM-BF<sub>4</sub>)-coated silver catalyst in an aqueous solution of EMIM-BF<sub>4</sub>. One of the surprises in the previous paper was that the selectivity to CO was better than 96% on silver, compared with ~80% in the absence of ionic liquid. In this article, we use sum frequency generation (SFG) to explore the mechanism of the enhancement of selectivity. The study used platinum rather than silver because previous workers had found that platinum is almost inactive for CO production from CO<sub>2</sub>. The results show that EMIM-BF<sub>4</sub> has two effects: it suppresses hydrogen formation and enhances CO<sub>2</sub> conversion. SFG shows that there is a layer of EMIM on the platinum surface that inhibits hydrogen formation. CO<sub>2</sub>, however, can react with the EMIM layer to form a complex such as CO<sub>2</sub>-EMIM at potentials more negative than -0.1 V with respect to a standard hydrogen electrode (SHE). That complex is converted to adsorbed CO at cathodic potentials of -0.25 V with respect to SHE. These results demonstrate that adsorbed monolayers can substantially lower the barrier for CO<sub>2</sub> conversion on platinum and inhibit hydrogen formation, opening the possibility of a new series of metal/organic catalysts for this reaction.



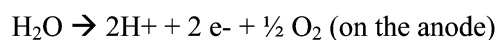
## INTRODUCTION

In artificial photosynthesis, there has been considerable progress on water splitting<sup>1–13</sup> using solar energy or solar-derived electricity, but CO<sub>2</sub> activation has proven to be more difficult.<sup>14–16</sup> According to a recent DOE report,<sup>1</sup> “electron conversion efficiencies of greater than 50% can be obtained, but at the expense of very high overpotentials (~1.5 V)”. This corresponds to a cell potential of 2.7 to 3.4 V.

In a recent paper,<sup>17</sup> we examined CO<sub>2</sub> conversion to CO in a dual compartment cell, with silver and 18 mol % 1-ethyl-3-methylimidazolium tetrafluoroborate (EMIM-BF<sub>4</sub>) in water in the cathode compartment and platinum with 0.5 M sulfuric acid in the anode compartment. We found that on silver CO<sub>2</sub> was converted to CO at applied cell voltages as small as 1.5 V. This compares to a thermodynamic potential for the gas-phase reaction CO<sub>2</sub> ⇌ CO + 1/2 O<sub>2</sub> of 1.33 V. We proposed that the overall reaction was as shown in Scheme 1, with protons diffusing from the anode to the cathode to complete the electrochemical reaction.

The rate-limiting step in the reduction of CO<sub>2</sub> is the one electron transfer to CO<sub>2</sub> to form a high-energy intermediate. We proposed that the ionic liquid provided a low-energy pathway for CO production, as illustrated in Figure 1.

## Scheme 1



One of the surprises in the previous work was that the selectivity for CO<sub>2</sub> production in an aqueous solution containing 18% by mole of EMIM-BF<sub>4</sub> was over 98%. By comparison, silver shows ~80% selectivity in the absence of the ionic liquid.<sup>16</sup> The object of this work is to determine why the selectivity enhancement occurs and determine what happens on the cathode catalyst that leads to conversion at low overpotential. In particular, we wished to combine electrochemical measurements with a recently developed compact broadband multiplex sum frequency generation (SFG) spectroscopy apparatus<sup>18</sup> to understand the mechanism of the process.

Received: November 2, 2011

Revised: June 20, 2012

Published: June 20, 2012

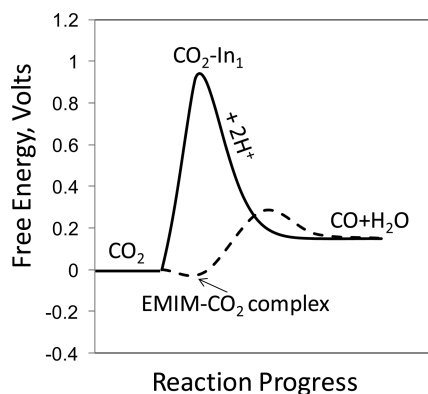


**Figure 1.** Schematic of how the free energy of the system changes during the reaction  $2\text{CO}_2 + 2\text{H}^+ + 2\text{e}^- \rightarrow \text{CO} + \text{H}_2\text{O}$  in water or acetonitrile (solid line) or EMIM- $\text{BF}_4$  (dashed line). The label  $\text{CO}_2\text{-In}_1$  refers to the intermediate that forms when the first electron is transferred during the reaction.

We choose platinum for these experiments. Previous workers found that platinum is inactive for  $\text{CO}_2$  conversion in aqueous solutions. Instead, only hydrogen production is observed.<sup>16</sup> Therefore, it was a case where enhancements in  $\text{CO}_2$  production could be easily observed. We find that indeed CO is formed on platinum in the presence of the ionic liquid and that the rate of hydrogen production is lower in EMIM  $\text{BF}_4$  compared with aqueous systems.

## EXPERIMENTAL SECTION

**Electrochemistry.** Electrochemistry was performed using a Solatron SI 1287 attached to a PC using CorrWare software. All of the experiments were conducted in a custom-made glass electrochemical cell shown schematically in Figure S1 of the Supporting Material. The working electrode was a 5 mm diameter platinum plug, and the counter electrode was made of a  $25 \times 25$  mm piece of size 52 platinum gauze. Reference electrodes were made using 0.01 M silver nitrate in acetonitrile. The reference electrode was contained by a 0.6 mm OD 7.5 cm long glass tube with a 1/8" long porous Vycor tip. The Vycor tip was held to the glass capillary by heat shrink. The reference electrode was made by placing the silver wire (99.9%) into the capillary filled with silver nitrate in acetonitrile. All water used in either experimentation, preparation, or cleaning, came from a DirectQ Millipore water purifier with an R-O filter (0.22  $\mu\text{m}$ , SN: 0328). The water from this system measures a resistance of 18.2 M $\Omega$ . Prior to using any of the ionic liquids, they were placed in a 250 mL flask and heated to 105  $^\circ\text{C}$  under a  $-23$ "Hg vacuum for at least 24 h. After this water removal, the water content was accessed qualitatively by comparing cyclic voltammetry and qualitatively through a Karl Fischer (KF) titration.

To monitor the reduction of carbon dioxide dissolved in the electrolyte solution, linear sweep voltammograms (LSVs) were taken both before and after the addition of carbon dioxide to the electrolyte solution. The electrolyte was sparged (150 sccm) with UHP argon for 2 h to remove any residual moisture and oxygen to establish a "blank". During the blank measurement, the ionic liquid was under an argon atmosphere (ca. 1 atm). To condition electrochemically the surface of the working electrode, 40 cyclic voltammogram (CV) cycles were applied at 50 mV/s between  $-2.0$  V and  $+0.5$  mV versus Ag/Ag<sup>+</sup> reference electrode described above. Linear sweep

measurements were taken at a scan rate of 10 mV/s in a stepped sweep mode with a 2 Hz low pass filter and IR compensation.

After a stable "blank" was established, carbon dioxide was then sparged (50 sccm) into the ionic liquid for 45 min. The LSV experiments for the carbon dioxide saturated experiments followed the same specifications as the blank, except for the head atmosphere, which was carbon dioxide rather than UHP argon. Figure S3 in the Supporting Information show this work for  $\text{CO}_2$  reduction on a Pt cathode.

**Sum Frequency Generation Spectroscopy.** The electrochemical cell for synchronized SFG and electrochemical experiments is composed of a Kel-F base with a glass cylinder attached to the top part of the Kel-F base. A glass plunger that holds the polycrystalline Pt working electrodes of 6 mm diameter is introduced through the glass cylinder and the Kel-F base. A  $\text{CaF}_2$  optical window forms the bottom of the Kel-F base, whereas a 50  $\mu\text{m}$  Teflon spacer provides a well-defined gap between the  $\text{CaF}_2$  window and the working electrode. This geometry allows for voltammetric scans at sweep rates of  $\leq 5$  mV/s without the detriment of strong ohmic drop effects that are associated with thin-layer electrochemistry. Cyclic voltammograms synchronized with SFG scans were recorded with a Princeton Applied Research (PAR 263A) potentiostat using a polycrystalline Pt wire as counter electrode and a Ag/Ag<sup>+</sup> reference electrode that was calibrated to the ferrocene redox couple.

A  $\text{CaF}_2$  optical window that is separated from the working electrode by a 50  $\mu\text{m}$  Teflon spacer allows the laser beams to probe the electrode–electrolyte interface. This enables us to synchronize the acquisition of the SFG spectra of the interface with the voltammetric scans. For the SFG experiments, tunable broadband infrared (BBIR) pulses were generated in an optical parametric amplifier (Light Conversion; Topas) pumped by a femtosecond Ti:sapphire laser system (Quantronix; Integra C series) at a repetition rate of 1 kHz. The BBIR pulses had pulse durations of  $\sim 120$  fs, typical bandwidths  $\Delta > 150$   $\text{cm}^{-1}$  and pulse energies of  $\sim 10$  and 13  $\mu\text{J}$  at frequencies  $\Omega$  of 2083 and 2350  $\text{cm}^{-1}$ , respectively. Narrowband visible pulses with 5  $\mu\text{J}$  pulse energy and a fixed wavelength of 800 nm were generated by narrowing the femtosecond pulses to a bandwidth of  $< 10$   $\text{cm}^{-1}$  with a Fabry–Pérot etalon. The visible pulse energy was reduced to 2.5  $\mu\text{J}$  while probing the CO vibrational bands (at an IR wavelength of 2083  $\text{cm}^{-1}$ ) to prevent laser-induced desorption of the CO from the electrode surface. The narrowband visible and BBIR pulses were overlapped in time and space on the electrode–electrolyte interface at an incident angle of  $\sim 60^\circ$  to the normal. Sum-frequency photons were collected with a spectrograph and a charge-coupled device (CCD) with the SFG, visible, and IR photons all being p-polarized.

## RESULTS AND DISCUSSION

Figure 2 shows an SFG spectrum of adsorbed EMIM taken in the presence and absence of  $\text{CO}_2$ . Two SFG peaks are observed; a  $\text{CH}_3$  bending mode at  $\sim 1430$  and a ring stretching mode at  $\sim 1570$   $\text{cm}^{-1}$ . These peaks are present whether the liquid is saturated with argon or carbon dioxide, and the peak positions do not vary over the potential range of interest ( $-2$  to  $+0.6$  V with respect to RHE). Interestingly, the peaks are more intense when less than 2/3 of a monolayer of CO is adsorbed on the surface. The selection rules for SFG are such that one could only observe EMIM if it was on or near the surface, and

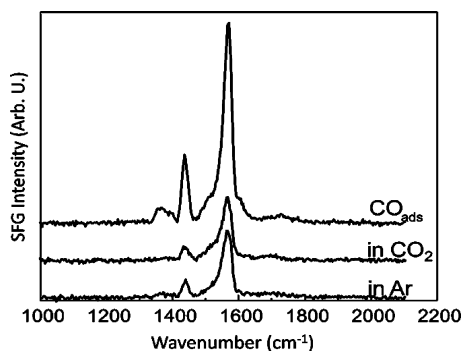


**Figure 2.** SFG spectra of a platinum catalyst in EMIM-BF<sub>4</sub> at  $-0.8$  V versus SHE in argon and CO<sub>2</sub> and in the presence of 2/3 of a monolayer of CO. The spectrum was taken for 50 s with a 4.0 uJ visible beam of 800 nm and an IR beam of 6300 nm. The spectra are offset on the y axis to emphasize the differences.

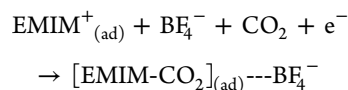
the observation that the intensity of the peaks changes when a small quantity of CO adsorbs would only occur if the EMIM was adsorbed on the surface. Therefore, we conclude that the platinum is partially or completely covered by EMIM under all conditions considered here.

Next, we wished to ask whether the monolayer of EMIM could change the reaction. Figure 3 shows a LSV of CO<sub>2</sub> conversion. There are two curves. One with an argon background and one where CO<sub>2</sub> is bubbled through the EMIM to create a solution that contains 100 mM CO<sub>2</sub> and 90 mM water. We observe some current in the absence of CO<sub>2</sub> due to water electrolysis, but the current increases substantially when CO<sub>2</sub> is added to the mixture. Notice that CO<sub>2</sub> conversion

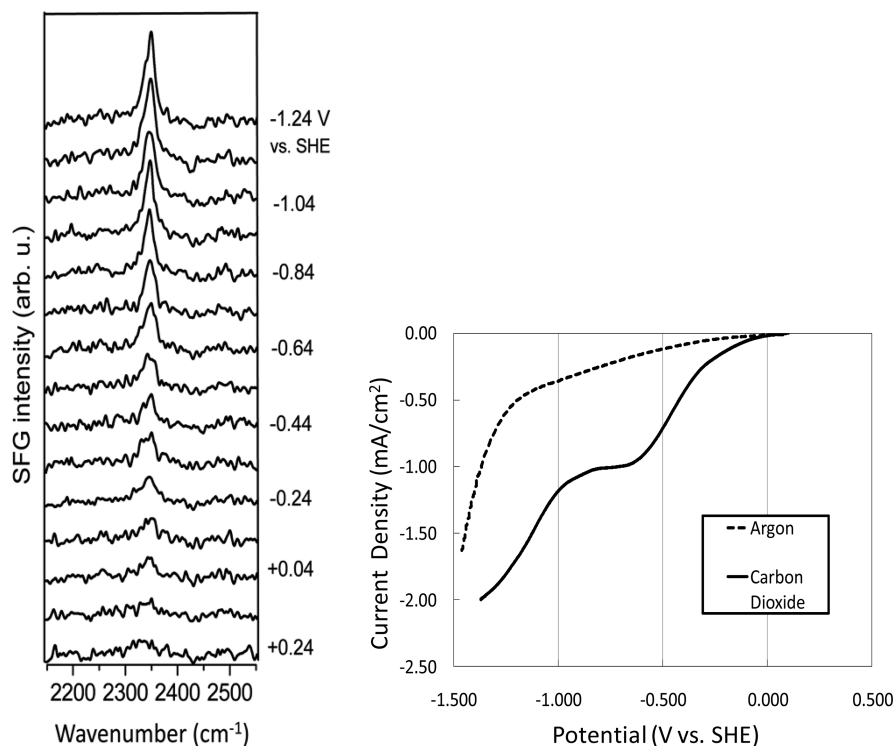
starts at about  $-0.25$  V with respect to a standard hydrogen electrode (SHE). By comparison, no CO conversion is observed at potentials more negative than  $-0.8$  V in the absence of the EMIM. Clearly the adsorbed EMIM has lowered the overpotential for the reaction.

Figure 3 also shows a series of SFG spectra taken during CO<sub>2</sub> electrolysis in EMIM-BF<sub>4</sub>. At cathode potentials more positive than  $+0.04$  V with respect to a SHE, we observe only a broad peak due to nonresonant contribution from the platinum surface.<sup>19,20</sup> However, as the cathode potential moves negative, a new narrow peak appears at  $2340$  cm<sup>-1</sup>. Simultaneously, LSV in Figure 3 shows that current is flowing into the solution. Because of the presence of 90 mM water in the electrolyte, the source of current is partially the reduction of water. We find that at most 15% of the difference current (between the argon-saturated curve and CO<sub>2</sub>-saturated curve) is due to the acceleration of water reduction in the presence of carbon dioxide, and thus a majority of the current flowing into solution can be attributed to CO<sub>2</sub> reduction processes.

We attribute the peak at  $2348$  cm<sup>-1</sup> to the formation of an EMIM-CO<sub>2</sub>---BF<sub>4</sub> complex via



Note that we do not know the electronic structure of the complex in the reaction above, but one possibility is the formation of a neutral [EMIM-CO<sub>2</sub>] or fluorinated EMIM-CO<sub>2</sub> complex (i.e., EMIM<sup>+</sup> has been converted to a neutral species when it combines with CO<sub>2</sub>). The subscript (ad) refers to adsorbed species.



**Figure 3.** Series of SFG spectra taken during CO<sub>2</sub> electrolysis in EMIM-BF<sub>4</sub> containing 90 mM water (left). Linear sweep voltammogram of three electrode cell taken simultaneously with SFG spectra (right). The current in the “argon” spectrum is attributed to reduction residual water in our EMIM-BF<sub>4</sub> because pure EMIM-BF<sub>4</sub> has been reported to be stable between  $+2$  and  $-2$  V versus SHE, and the residual current varies with the water concentration.

Figure 3 shows that the new species has a stretching frequency of  $2348\text{ cm}^{-1}$ . By comparison, gas-phase  $\text{CO}_2$  shows a stretching frequency of  $2396\text{ cm}^{-1}$ .<sup>21</sup> Thus, it appears that new species contains  $\text{CO}_2$ . The species cannot simply be an adsorbed  $\text{CO}_2$  molecule. (If the  $\text{CO}_2$  were directly bound to the platinum in a bidentate configuration, then the frequency of the  $\text{CO}_2$  would shift to considerably lower frequencies while linear  $\text{CO}_2$  was not SFG-active.) For  $\text{CO}_2$  to be SFG-active, it must be present in an environment that imbues both IR and Raman activity to its vibrational transitions and the environment must exhibit noncentrosymmetric order on scales comparable to a visible wavelength. (The signal is therefore not  $\text{CO}_2$  in the bulk due to inversion symmetry.) If  $\text{CO}_2$  were attached or complexed with an imidazole ring, then  $\text{CO}_2$  vibrations would be both IR- and Raman-active,<sup>22</sup> but the  $\text{CO}_2$  stretching frequency would only be slightly perturbed.

It is also interesting to notice that the size of the EMIM- $\text{CO}_2$  peak grows linearly as the potential is swept from  $-0.2$  to  $-0.6$  V, levels off, and then starts to grow again below  $-0.8$  V. The current due to  $\text{CO}_2$  conversion follows the same trend. This suggests that EMIM- $\text{CO}_2$  is a key intermediate in the conversion of  $\text{CO}_2$  to CO.

The next question is whether the complex is reactive or whether it has been stabilized so much that it became unreactive. SFG was also used to examine that possibility. Figure 4 shows the CO region of the spectrum during

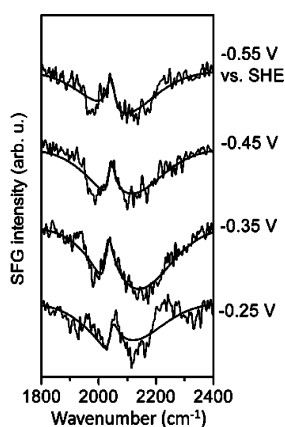


**Figure 4.** Series of SFG spectra taken by cycling the potential from open cell to the potential shown and repeating 40 times to allow for CO buildup. The spectra have been inverted.

experiments similar to those in Figure 3. In this experiment, we cycled the potential. This allowed us to overcome some of the mass-transfer limitations in our cell.

There is a broad peak due to the nonresonant susceptibility and a narrower vibrational band due to adsorbed CO. The CO transition starts at  $2050\text{ cm}^{-1}$  and shifts down to  $2040\text{ cm}^{-1}$  due to the Stark effect.<sup>23,24</sup> In data not shown, it shifts up again due to dipole interactions as the CO coverage increases.<sup>25–28</sup> All of these behaviors are as expected for CO formation on platinum.

Figure 4 demonstrates that CO buildup is observed whenever the electrode was repetitively cycled down to a potential of  $-0.25$  V with respect to SHE. After 40 cycles, the peak intensity is similar to that for a monolayer of CO. By comparison, CO buildup on platinum is not normally observed until the potential is below  $-1.1$  V.<sup>16</sup> Therefore, it appears that

the conversion of  $\text{CO}_2$  to CO can occur at much less negative potentials in our system than have been previously observed.

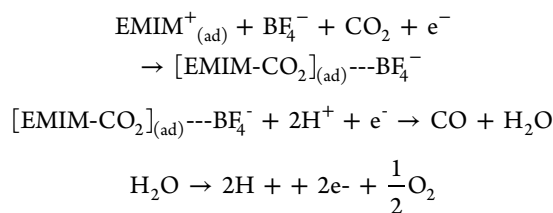
We have also observed continuous gas-phase CO production and oxygen formation in the gas phase by heating the platinum catalyst to  $110\text{ }^\circ\text{C}$ . We continued the reaction for 7900 turnovers over 4 h. Furthermore, the reaction still occurs when we separate the anode and cathode with a proton-conducting Nafion membrane. Figure 4 shows that  $\text{CO}_2$  is reduced to CO at a cell potential of 2.5 V. We also see the reduction of water (absorbed in the ionic liquid) to hydrogen gas under these conditions. The faradaic efficiency for CO was 17% whereas the faradaic efficiency for  $\text{H}_2$  was 80%.

It is useful to consider the implication of the results here. First, the ionic liquid has activated the catalyst for the production of carbon monoxide. Previous workers did not observe significant CO production on platinum significant CO production on platinum under conditions similar to those reported here. Therefore, the ionic liquid has been able to catalyze the formation of CO on platinum, in a similar way to the way observed on silver. Beyond that, the ionic liquid suppressed the formation of hydrogen.

The spectroscopic results also provide evidence in support of the mechanism we previously proposed. Years ago Bockris and coworkers<sup>29,30</sup> proposed that high overpotentials are needed to convert  $\text{CO}_2$  because the equilibrium potential for the formation of the intermediate that forms when the first electron is transferred is very negative in water and in most common solvents. Bockris called this intermediate “ $\text{CO}_2^-$ ”. In this context, the term “ $\text{CO}_2^-$ ” is not necessarily a bare  $\text{CO}_2^-$  anion. Instead, it is whatever species forms when the first electron is transferred during the reaction. In fact, Lamy et al.<sup>31</sup> found that the equilibrium potential for  $\text{CO}_2^-$  formation is  $-2.1$  V versus SCE in dimethylformamide (DMF), so it is unlikely that the species is  $\text{CO}_2^-$ . Because of the negative equilibrium potential, one needs to run the cathode very negative (i.e., at a high overpotential) for the reaction to occur. This is very energy inefficient. See Figure 1. Metals lower the needed potential, but still, Chandrasekaran and Bockris suggested that in acetonitrile doped with tetraammonium the first species does not start to form on platinum until the potential is below  $-0.8$  V with respect to SHE.

Notice that we observe what we interpret as being a  $\text{CO}_2$  intermediate complex at  $-0.14$  V with respect to SHE. The peak grows as the potential is lowered to  $-0.8$  V. We also observe significant current between  $-0.2$  and  $-0.8$  V. This compares to a negligible difference between the current in  $\text{CO}_2$  and in argon in the absence of the ionic liquid. Evidently, the ionic liquid is stabilizing the  $(\text{CO}_2)$ -intermediate, as indicated in Figure 1. This can lead to a lower energy pathway, as indicated in Figure 1. Whereas there would still be a barrier to form the final products of the reaction, the overall barrier to reaction would be reduced.<sup>32</sup>

Therefore, our data are consistent with the idea that the adsorbed EMIM- $\text{BF}_4$  acts as a cocatalyst for  $\text{CO}_2$  conversion via the mechanism:



It is useful to compare the mechanism above to the mechanism for CO<sub>2</sub> conversion in pyridine previously proposed by Barton et al.<sup>33</sup> and Morris et al.<sup>34</sup> Barton et al.<sup>33</sup> and Morris et al.<sup>34</sup> proposed that CO<sub>2</sub> conversion is a homogeneous reaction. First pyridinium radicals accumulate in solution when pyridine is held at negative potentials. CO<sub>2</sub> then reacts homogeneously with the pyridinium radicals to yield products.

This differs from our proposal in that we propose that the reaction is heterogeneous not homogeneous and that the catalyst is a combination of EMIM and metal. EMIM first adsorbs. Then, the EMIM–metal complex catalyzes the formation of CO via a [EMIM-CO<sub>2</sub>]<sub>(ad)</sub> intermediate. Note that we have found that the rate of reaction is quite different on platinum than on silver, which is strong evidence that the reaction is homogeneous not heterogeneous.

We have no evidence of formation of a EMIM radical in solution over the conditions of our experiment. Previous workers<sup>35,36</sup> have reported that pure EMIM-BF<sub>4</sub> is electrochemically stable over all of the conditions used here. No radicals form at potentials between -0.2 and -2 V.<sup>35,36</sup> We observe modest currents in Figure 2 even in the absence of CO<sub>2</sub>, but those currents are due to the small amounts of water (~80 mM) that remain in EMIM BF<sub>4</sub> even after the EMIM BF<sub>4</sub> is dried. Therefore, it is unlikely that an EMIM radical could form in solution during experiments.

Furthermore, in unpublished data, we have found that the reaction rate varies significantly with the metal. One would not expect such an effect unless the metal was playing an active role in the reaction.

In summary, in this article, we showed that a bifunctional catalyst consisting of a metal, platinum, and an adsorbed cation, EMIM<sup>+</sup><sub>(ad)</sub>, is active for CO<sub>2</sub> conversion to CO at low overpotentials. The reaction seems to occur via formation of an adsorbed CO<sub>2</sub>-EMIM complex, leading to a low-energy pathway. This result demonstrates the potential of bifunctional catalysts consisting of bulk metals and adsorbed cationic species for CO<sub>2</sub> conversion.

## ■ ASSOCIATED CONTENT

### ● Supporting Information

Details of the experimental procedures, calibration of the reference electrodes, supplemental stripping spectra, and GC traces showing CO formation. This material is available free of charge via the Internet at <http://pubs.acs.org>.

## ■ AUTHOR INFORMATION

### Corresponding Author

\*E-mail: [rich.masel@dioxidematerials.com](mailto:rich.masel@dioxidematerials.com).

### Notes

R.M. and B.R. have submitted several patents that are related to the material in this paper. RM is also an owner that is commercializing related technology. The other authors declare no competing financial interest.

## ■ ACKNOWLEDGMENTS

This work was partially supported by the Department of Energy under grant DE-SC0004453 and by Dioxide Materials. Any opinions, findings, and conclusions or recommendations expressed in this manuscript are those of the authors and do not necessarily reflect the views of the Department Of Energy. R.I.M. and B.A.R. have submitted multiple patents based on the

work. The SFG measurements in their early stages were supported by the Air Force Office of Scientific Research under contract FA9550-09-1-0163, and in the later stages, Prabuddha Mukherjee was supported by the Center for Electrical Energy Storage - Tailored Interfaces, an Energy Frontier Research Center funded by the U.S. Department of Energy, Office of Science, Office of Basic Energy Sciences under award number DE-AC02-06CH11357 subcontract 9F-31921. B.B. thanks the Alexander von Humboldt foundation for support.

## ■ REFERENCES

- (1) Bell, A. T. *Basic Research Needs, Catalysis For Energy*; U.S. Department of Energy report PNNL17214; U.S. Department Of Energy: Bethesda, MD, 2008; [www.anl.gov/catalysis-science/publications/CAT\\_rpt.pdf](http://www.anl.gov/catalysis-science/publications/CAT_rpt.pdf).
- (2) Hammarstrom, L.; Hammes-Schiffer, S. *Acc. Chem. Res.* **2009**, *42*, 1859–1860.
- (3) Lewis, N. S.; Nocera, D. G. *Proc. Natl. Acad. Sci. U. S. A.* **2006**, *103* (43), 15729–15735.
- (4) Lewis, N. S. *Science* **2007**, *315*, 798–801.
- (5) Lewis, N. S. *ChemSusChem* **2009**, *2*, 383–386.
- (6) Rakowski, D. M.; Dubois, D. L. *Acc. Chem. Res.* **2009**, *42*, 1974–1982.
- (7) Vincenzo, B.; Alberto, C.; Margherita, V. *ChemSusChem* **2008**, *1*, 26–58.
- (8) Blankenship, R. E.; Tiede, D. M.; Barber, J.; Brudvig, G. W.; Fleming, G.; Ghirardi, M.; Gunner, M. R.; Junge, W.; Kramer, D. M.; Melis, A.; et al. *Science* **2011**, *332*, 805–809.
- (9) Cogdell, R. J.; Brotsudarmo, T. H. P.; Gardiner, A. T.; Sanchez, P. M.; Cronin, L. *Biofuels* **2010**, *1*, 861–876.
- (10) Hoffmann, M. R.; Moss, J. A.; Baum, M. M. *Dalton Trans.* **2011**, *40*, S151–S158.
- (11) Inoue, H.; Shimada, T.; Kou, Y.; Nabetani, Y.; Masui, D.; Takagi, S.; Tachibana, H. *ChemSusChem* **2011**, *4*, 173–179.
- (12) Michl, J. *Nat. Chem.* **2011**, *3*, 268–269.
- (13) Zhou, H.; Fan, T.; Zhang, D. *ChemCatChem* **2011**, *3*, 513–528.
- (14) DuBois, D. L. *Encycl. Electrochem.* **2006**, *7a*, 202–225.
- (15) Gattrell, M.; Gupta, N.; Co, A. J. *Electroanal. Chem.* **2006**, *594*, 1–19.
- (16) Hori, Y. *Mod. Aspects Electrochem.* **2008**, *42*, 89–189.
- (17) Rosen, B. A.; Salehi-Khojin, A.; Thorson, M. R.; Zhu, W.; Whipple, D. T.; Kenis, P. J. A.; Masel, R. I. *Science* **2011**, *334*, 643–644.
- (18) Lagutchev, A.; Lozano, A.; Mukherjee, P.; Hambir, S. A.; Dlott, D. *Spectrochim. Acta, Part A* **2010**, *75*, 1289.
- (19) Baldelli, S.; Gewirth, A. A. *Adv. Electrochem. Sci. Eng.* **2006**, *9*, 163–198.
- (20) Carter, J. A.; Wang, Z.; Dlott, D. D. *Acc. Chem. Res.* **2009**, *42*, 1343–1351.
- (21) Bailey, C. R. *Nature (London, U. K.)* **1929**, *123*, 410.
- (22) Bhargava, B. L.; Saharay, M.; Balasubramanian, S. *Bull. Mater. Sci.* **2008**, *31*, 327–334.
- (23) Chang, S. C.; Jiang, X.; Roth, J. D.; Weaver, M. J. *J. Phys. Chem.* **1991**, *95*, 5378–5382.
- (24) Jiang, X.; Weaver, M. J. *Surf. Sci.* **1992**, *275*, 237–252.
- (25) Banholzer, W. F.; Masel, R. I. *Surf. Sci.* **1984**, *137*, 339–360.
- (26) Olsen, C. W.; Masel, R. I. *Surf. Sci.* **1988**, *201*, 444–60.
- (27) Banholzer, W. F.; Parise, R. E.; Masel, R. I. *Surf. Sci.* **1985**, *155*, 653–666.
- (28) Wang, J.; Masel, R. I. *J. Catal.* **1990**, *126* (2), 519–531.
- (29) Bockris, J. O. M.; Wass, J. C. J. *Electrochem. Soc.* **1989**, *136*, 2521–2528.
- (30) Chandrasekaran, K.; Bockris, J. O. M. *Surf. Sci.* **1987**, *185*, 495–514.
- (31) Lamy, E.; Nadjo, L.; Saveant, J. M. *J. Electroanal. Chem. Interfacial Electrochem.* **1977**, *78*, 403–407.
- (32) Masel, R. I. *Chemical Kinetics and Catalysis*. Wiley: New York, 2001.

(33) Barton, C. E.; Lakkaraju, P. S.; Rampulla, D. M.; Morris, A. J.; Abelev, E.; Bocarsly, A. B. *J. Am. Chem. Soc.* **2010**, *132*, 11539–11551.

(34) Morris, A. J.; McGibbon, R. T.; Bocarsly, A. B. *ChemSusChem* **2011**, *4*, 191–196.

(35) Fuller, J.; Breda, A. C.; Carlin, R. T. *J. Electroanal. Chem.* **1998**, *459*, 29–34.

(36) Fuller, J.; Carlin, R. T.; Osteryoung, R. A. *J. Electrochem. Soc.* **1997**, *144*, 3881–3886.